

Discovery and Characterization of a Peptide That Enhances Endosomal Escape of Delivered Proteins in Vitro and in Vivo

Margie Li,[†] Yong Tao,[‡] Yilai Shu,^{‡,§,||} Jonathan R. LaRoche,[‡] Angela Steinauer,[#] David Thompson,[†] Alanna Schepartz,^{#,⊥} Zheng-Yi Chen,[‡] and David R. Liu^{*,†,∇}

[†]Department of Chemistry & Chemical Biology, Harvard University, 12 Oxford Street, Cambridge, Massachusetts 02138, United States

[‡]Department of Otolaryngology and Program in Neuroscience, Harvard Medical School and Eaton Peabody Laboratory, Massachusetts Eye and Ear Infirmary, Boston, Massachusetts 02114, United States

[§]Department of Otolaryngology and Skull Base Surgery, Eye, Ear, Nose and Throat Hospital, Shanghai Medical College, Fudan University, Shanghai 200031, China

^{||}Key Laboratory of Hearing Medicine, Ministry of Health, Shanghai, 200031, China

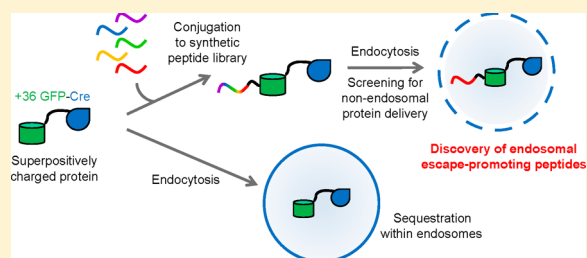
[⊥]Department of Molecular, Cellular and Developmental Biology, Yale University, New Haven, Connecticut 06520-8107, United States

[#]Department of Chemistry, Yale University, New Haven, Connecticut 06520-8107, United States

[∇]Howard Hughes Medical Institute, Harvard University, 12 Oxford Street, Cambridge, Massachusetts 02138, United States

Supporting Information

ABSTRACT: The inefficient delivery of proteins into mammalian cells remains a major barrier to realizing the therapeutic potential of many proteins. We and others have previously shown that superpositively charged proteins are efficiently endocytosed and can bring associated proteins and nucleic acids into cells. The vast majority of cargo delivered in this manner, however, remains in endosomes and does not reach the cytosol. In this study we designed and implemented a screen to discover peptides that enhance the endosomal escape of proteins fused to superpositively charged GFP (+36 GFP). From a screen of peptides previously reported to disrupt microbial membranes without known mammalian cell toxicity, we discovered a 13-residue peptide, aurein 1.2, that substantially increases cytosolic protein delivery by up to ~5-fold in a cytosolic fractionation assay in cultured cells. Four additional independent assays for nonendosomal protein delivery collectively suggest that aurein 1.2 enhances endosomal escape of associated endocytosed protein cargo. Structure–function studies clarified peptide sequence and protein conjugation requirements for endosomal escape activity. When applied to the in vivo delivery of +36 GFP–Cre recombinase fusions into the inner ear of live mice, fusion with aurein 1.2 dramatically increased nonendosomal Cre recombinase delivery potency, resulting in up to 100% recombined inner hair cells and 96% recombined outer hair cells, compared to 0–4% recombined hair cells from +36-GFP-Cre without aurein 1.2. Collectively, these findings describe a genetically encodable, endosome escape-enhancing peptide that can substantially increase the cytoplasmic delivery of cationic proteins in vitro and in vivo.



INTRODUCTION

Proteins that bind extracellular targets, including monoclonal antibodies,¹ Fc fusions,² and cytokines,³ have served as important therapeutics.⁴ Fully realizing the therapeutic potential of proteins, however, requires methods to enable exogenous proteins to access intracellular targets. Because the vast majority of proteins cannot spontaneously cross cell membranes, the development of intracellular protein delivery methods could facilitate applications including enzyme replacement therapies for metabolic diseases,⁵ transcription factor-driven changes in cell fate,⁶ and genome editing.⁷

Several methods for protein delivery have been explored in the past decade, including cell-penetrating peptides (CPPs),⁸

penta-arg proteins,⁹ receptor ligands,¹⁰ and lipid nanoparticles.¹¹ While these and other methods have advanced the field of protein delivery, challenges including cytotoxicity, lack of generality, low potency, or poor in vivo activity continue to limit their therapeutic relevance.^{12,13}

We previously reported the discovery of superpositively charged proteins, a class of engineered and naturally occurring proteins that have abnormally high net positive charge, and their ability to potently deliver proteins and nucleic acids into mammalian cells.^{14–17} While superpositive proteins are very

Received: June 3, 2015

Published: October 14, 2015

efficiently endocytosed^{18,19} and can be more effective for protein delivery than CPPs,¹⁵ the vast majority of endocytosed proteins remain sequestered in endosomes¹⁸ that either mature into lysosomes, resulting in protein degradation, or are recycled to the surface of the cell,²⁰ resulting in extracellular protein release (Figure 1A). As a result, relatively high concentrations

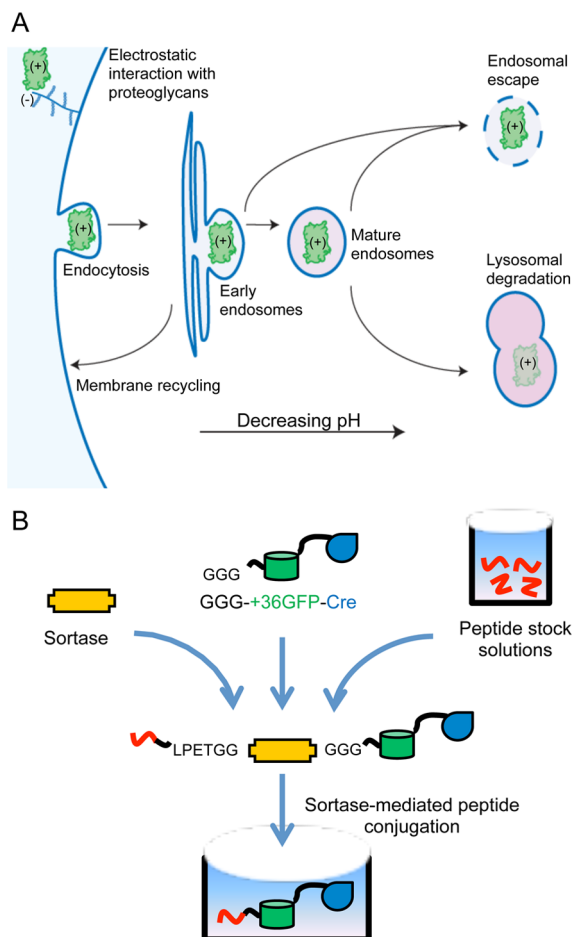


Figure 1. (A) Overview of protein delivery in mammalian cells. Cationic macromolecules such as +36 GFP interact with anionic sulfated proteoglycans on the cell surface and are endocytosed and sequestered in early endosomes. The early endosomes can acidify into late endosomes or lysosomes. Alternatively, early endosomes may be trafficked back to the cell surface as part of the membrane-recycling pathway. To access the cytoplasm, an exogenous cationic protein must escape endosomes before it is degraded or exported. (B) Sortase-mediated conjugation of peptides with +36 GFP–Cre recombinase prior to screening. Sortase was used to conjugate synthetic peptides containing a C-terminal LPETGG with expressed +36 GFP–Cre containing an N-terminal GGG. The resulting peptide–LPETGGG–+36 GFP–Cre fusion proteins have the same chemical composition as expressed recombinant proteins, but are more easily assembled.

(μM) of exogenous protein are typically needed for modest cytosolic or nuclear delivery. Although superpositively charged proteins can slow endosomal maturation,¹⁸ the inefficiency of endosomal escape enables only a small fraction of delivered protein to reach the cytosol.²¹

To address this protein delivery bottleneck, we sought to discover peptides that facilitate endosomal escape when fused to endocytosed superpositively charged proteins such as +36 GFP. Membrane-active peptides such as influenza-derived HA2

have been reported to be endosomolytic.²² However, many of these peptides, including HA2, are cytotoxic at concentrations required for protein delivery.^{23,24} Antimicrobial peptides (AMPs) are a class of membrane-active peptides that penetrate microbial membranes to provide defense against bacteria, fungi, and viruses, often with high selectivity.²⁵ Given that many AMPs exhibit minimal toxicity to mammalian cells,²⁶ we hypothesized that the altered endosomal environment or endosomal membrane curvature could induce some AMPs to be endosomolytic without exhibiting significant mammalian cell toxicity at useful concentrations. To test this hypothesis, we performed a screen of AMPs for their ability to increase protein delivery into the cytosol.

A major challenge to developing agents that enhance endosomal escape is the lack of well-established assays that can distinguish proteins trapped in the endosomes from proteins released into the cytosol. Commonly used enzyme delivery assays involve substrates and products that can freely diffuse through membranes and cannot differentiate between endosomal and cytosolic proteins. To overcome this challenge, we used multiple independent assays that reflect the interaction of a variety of cargo with a variety of cytosolic targets to evaluate endosomal escape of AMP–protein fusions.

In this study, we discovered aurein 1.2 (GLFDIIKKIAESF) as a peptide that enhances the endosomal escape of a variety of cargo fused to +36 GFP. We elucidated structure–function relationships within aurein 1.2 using alanine scanning and mutational analysis. Results from three independent delivery assays confirmed that treatment of mammalian cells with cargo proteins fused to aurein 1.2–+36 GFP result in more efficient cytosolic delivery than the same proteins fused to +36 GFP alone. Finally, we describe the ability of aurein 1.2 to enhance nonendosomal protein delivery in vivo. Cre recombinase enzyme was delivered into hair cells in the cochlea (inner ear) of live mice with much greater (>20-fold) potency when fused with aurein 1.2 than in the absence of the peptide. These results together provide a simple molecular strategy for enhancing the cytosolic delivery of proteins in cell culture and in vivo that is genetically encoded, localized to cargo molecules, and does not require global treatment with cytotoxic small molecules.

RESULTS

Preparation of Antimicrobial Peptide Conjugates of Supercharged GFP–Cre Fusion Proteins. We sought AMPs from the Antimicrobial Peptide Database²⁷ that are ≤ 25 amino acids long (to facilitate their preparation and conjugation to +36 GFP), lack post-translational modifications, and are not known to be toxic to mammalian cells. Based on these criteria, we identified 36 AMPs ranging from 9 to 25 amino acids in length (Table 1). Each of the peptides was synthesized on solid phase with an LPETGG sequence appended to their C-terminus to enable sortase-catalyzed conjugation²⁸ (Figure 1B). Assembly of proteins using sortase proved more amenable to rapid screening than the construction and expression of the corresponding fusions, especially since several AMP fusions do not express efficiently in *E. coli*.

The peptides were conjugated to purified GGG–(+36 GFP)–Cre using our previously described evolved sortase A enzyme (eSrtA).²⁸ Sortase catalyzes the transpeptidation between a substrate containing the C-terminal LPETGG and a substrate containing an N-terminal glycine to form a native

Table 1. List of Peptides Chosen from the Antimicrobial Peptide Database (APD)^a

label	APD number	sequence	conjugation efficiency
A	AP00408	FLFPLITSFLSKVL	55%
B	AP00405-11	FISAIASMLGKFL	70%
C	AP00327	GWFDVVKHIASAV	–
D	AP01434	FFGSVLKLPKIL	–
E	AP00013	GLFDIIKIAESF	77%
F	AP00025	HGVSGHGQHGTVHG	20%
G	AP00094	FLPLIGRVLGSL	–
H	AP00012	GLFDIIKIAESI	28%
I	AP00014	GLLDIVKKVVGAFGSL	–
J	AP00015	GLFDIVKKVVGALGSL	13%
K	AP00016	GLFDIVKKVVGAGSL	–
L	AP00017	GLFDIVKKVVGTLGSL	18%
M	AP00018	GLFDIVKKVVGAFGSL	–
N	AP00019	GLFDIAKKVIGVIGSL	–
O	AP00020	GLFDIVKKIAGHIAGSI	–
P	AP00021	GLFDIVKKIAGHIASSI	–
Q	AP00022	GLFDIVKKIAGHIVSSI	–
R	AP00101	FVQWFSKFLGRIL	51%
S	AP00351	GLFDVIKKVASVIGGL	11%
T	AP00352	GLFDIIKKVASVVGGL	–
U	AP00353	GLFDIIKKVASVIGGL	4%
V	AP00567	VWPLGLVICKALKIC	4%
W	AP00597	NFLGTLVNLAKKIL	34%
X	AP00818	FLPLIGKILGTIL	14%
Y	AP00866	FLPIIAKVLGSL	86%
Z	AP00870	FLPIVGKLLSGLL	–
AA	AP00875	FLSSIGKILGNLL	88%
AB	AP00898	FLSGIVGMLGKLF	70%
AC	AP01211	TPFKLSLHL	81%
AD	AP01249	GILDAIKAIKAAG	20%
AE	AP00013-G	LFDIIKIAESF	63%
AF	AP00013-2x	LFDIIKIAESGFLFDIIKIAESF	–
AG	AP00722-75	GLLNLGLALRLGKRALKKIKRLCR	–
AH	His13	GHHHHHHHHHHHHHHH	–
AI	AP00512	FKCRRWQWRM	42%
AJ	AP00553	KTCENLADTY	–

^aPeptides were synthesized with a C-terminal LPETGG tag to enable conjugation with an evolved sortase (eSrtA). Conjugation efficiencies were calculated based on LC-MS results using peak abundance as determined through MaxEnt protein deconvolution.

peptide bond linkage and a protein identical to the product of translational fusion.

The efficiency of eSrtA-mediated conjugation varied widely among the peptides (Supporting Information Figure S1). Of the 36 peptides chosen for screening, 20 showed detectable (4% to 88%) sortase-mediated conjugation to +36 GFP–Cre, as observed by LC-MS, to generate desired peptide–LPETGGG–(+36 GFP)–Cre fusion proteins (Table 1). Unreacted peptide was removed by ultrafiltration with a 30-kD molecular weight cut off membrane.

Primary Screen for Endosomal Escape. We assayed the ability of each peptide–(+36 GFP)–Cre recombinase fusion when added to culture media to effect recombination in BSR.LNL.tdTomato cells,¹⁵ a hamster kidney cell line derived from BHK-21 (Supporting Information Figure S2). Because

Cre recombinase must enter the cell, escape endosomes, enter the nucleus, and catalyze recombination to generate tdTomato fluorescence, this assay reflects the availability of active, nonendosomal recombinase enzyme that reaches the nucleus. As a positive control, we treated cells with +36 GFP–Cre and chloroquine, a known endosome-disrupting small molecule.²⁹

The reporter BSR.LNL.tdTomato cells were incubated with 250 nM of each peptide–(+36 GFP)–Cre protein in serum-free media. In the absence of any conjugated peptide, treatment of reporter cells with 250 nM + 36 GFP–Cre protein resulted in 4.5% of the cells expressing tdTomato, consistent with previous reports.¹⁸ The same concentration of protein incubated with 100 μ M chloroquine as a positive control resulted in an average of 48% recombined cells (Figure 2). The

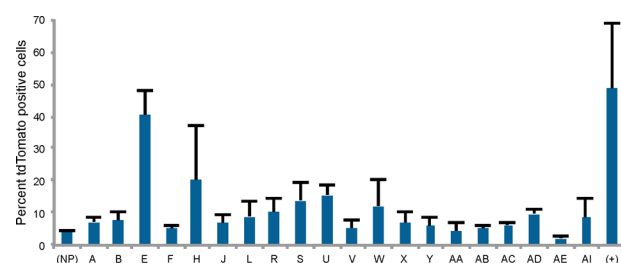


Figure 2. Primary screen for cytosolic delivery of Cre recombinase in BSR.LNL.tdTomato cells. Initial screen of 20 peptide–(+36 GFP)–Cre conjugated proteins. Cytosolic Cre delivery results in recombination and tdTomato expression. The percentage of tdTomato positive cells was determined by fluorescence image analysis. 250 nM +36 GFP–Cre was used as the no-peptide control (NP), and addition of 100 μ M chloroquine was used as the positive control (+). Cells were treated with 250 nM protein for 4 h in serum-free DMEM. Cells were washed and replated with full DMEM and incubated for 48 h. Error bars represent the standard deviation of three independent biological replicates.

results of chloroquine treatment varied substantially between independent replicates. As chloroquine is known to be toxic to cells above 100 μ M, we speculate that this variability arises from the small differences between chloroquine's efficacious and toxic dosages.

Ten of the screened peptide conjugates resulted in recombination efficiencies that were significantly above that of +36 GFP–Cre (Figure 2). The most potent functional delivery of Cre was observed with aurein 1.2–+36 GFP–Cre (Table 1, entry E). Treatment with aurein 1.2–+36 GFP–Cre resulted in an average of 40% recombined cells, comparable to that of the chloroquine positive control (Figure 2). To investigate the impact of differential conjugation efficiency on peptide performance, we compared citropin 1.3 (Table 1, entry U), which displayed a moderate level of recombination and the lowest level of conjugation (4%), to aurein 1.2, which has the highest level of recombination and also a high level of conjugation (77%).

Both aurein 1.2–+36 GFP–Cre and citropin 1.3–+36 GFP–Cre were cloned, expressed, and purified as fusion proteins. The recombination signal from treatment with 250 nM of expressed aurein 1.2–+36 GFP–Cre was 10.4-fold above that of +36 GFP–Cre. In contrast, treatment with 250 nM expressed citropin 1.3–+36 GFP–Cre did not induce any enhanced Cre delivery. When the treatment concentration was increased to 1 μ M, aurein 1.2–+36 GFP–Cre and citropin 1.3–+36 GFP–Cre resulted in 3.8-fold and 3.0-fold higher

recombination levels, respectively, than that of +36 GFP–Cre alone (Figure 3A). These results suggest that while aurein 1.2

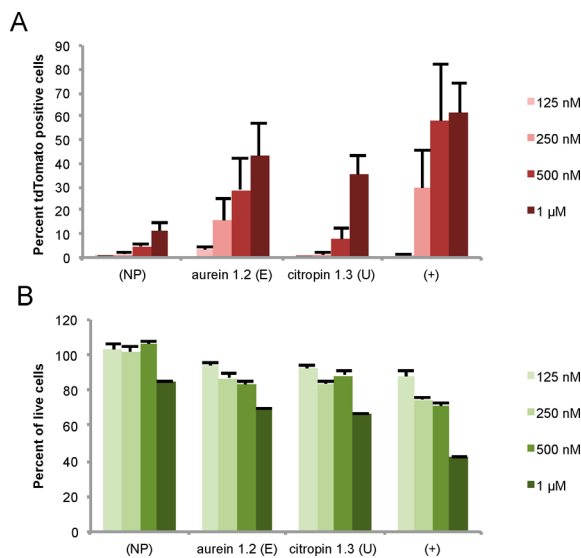


Figure 3. Efficacy and toxicity of recombinant expression fusions of aurein 1.2 (“E”) and citropin 1.3 (“U”). (A) Cytosolic Cre delivery results in recombination and tdTomato expression. The percentage of tdTomato positive cells was determined by flow cytometry. Protein fusions were delivered at 125 nM, 250 nM, 500 nM, and 1 μM. (B) Toxicity of aurein 1.2 and citropin 1.3 as determined by CellTiterGlo (Promega) assay. Protein fusions were delivered at 125 nM, 250 nM, 500 nM, and 1 μM. The labeled concentration of +36 GFP–Cre was used as the no peptide control (NP), and addition of 100 μM chloroquine was used as the positive control (+). Cells were treated with 250 nM protein for 4 h in serum-free media. Cells were washed and replated with full DMEM and incubated for 48 h. Error bars represent the standard deviation of three independent biological replicates.

and citropin 1.3 both enhance the delivery of functional, nonendosomal +36 GFP–Cre protein at high concentrations, aurein 1.2 has greater efficacy than citropin 1.3 at lower concentrations.

Next, we evaluated the toxicity of each fusion protein at a range of concentrations (125 nM to 1 μM) using an ATP-dependent cell viability assay at 48 h after treatment. For +36 GFP–Cre, we observed no cellular toxicity up to 1 μM treatment, which resulted in 85% viable cells. Cells treated with 250 nM recombinant aurein 1.2–+36 GFP–Cre and citropin 1.3–+36 GFP–Cre displayed 87% and 84% viability, respectively. Applying 1 μM treatments decreased cell viability to 70% and 66%, respectively (Figure 3B). In light of its activity and low cytotoxicity at 250 nM, we characterized in depth the ability of aurein 1.2 to enhance cytosolic protein delivery.

Site-Directed Mutagenesis of Aurein 1.2. Aurein 1.2 (GLFDIIKKIAESF) is a potent AMP excreted from the Australian tree frog, *Litoria aurea*.³⁰ Interestingly, citropin 1.3 (GLFDIIKKVASVIGGL) is a closely related peptide and is excreted from a different Australian tree frog, *Litoria citropa*.³¹ While the properties of aurein 1.2 have been investigated for its antibacterial and antitumorogenic abilities,³⁰ its ability to enhance endosomal escape or macromolecule delivery has not been previously reported. The free peptide is thought to adopt an amphipathic alpha helical structure in solution, but the length of the helix is too short to span a lipid bilayer.³² Therefore, it has been theorized that aurein 1.2 disrupts

membranes through a “carpet mechanism” in which peptides bind to the membrane surface in a manner that allows hydrophobic residues to interact with lipid tails and hydrophilic residues to interact with polar lipid head groups.³³ Above a critical concentration, the peptides are thought to alter the curvature of the membrane enough to break apart the compartment.

To identify the residues involved in enhancing non-endosomal protein delivery, we performed an alanine scan of the 13 amino acid positions of aurein 1.2 by cloning, expressing, and purifying each alanine mutant of aurein 1.2–+36 GFP–Cre. The resulting fusion proteins were assayed in BSR.LNL.tdTomato reporter cells as described above (Table 2). Seven positions were moderately to highly intolerant of

Table 2. Site-Directed Mutagenesis of Aurein 1.2^a

label	sequence
Aurein 1.2	GLFDIIKKIAESF
G1A	ALFDIIKKIAESF
L2A	GLFDIIKKIAESF
F3A	GLADIIKKIAESF
D4A	GLFAIIKKIAESF
I5A	GLFDIAIKKIAESF
I6A	GLFDIAKKIAESF
K7A	GLFDIIAKIAESF
K8A	GLFDIIKIAESF
I9A	GLFDIIKKAESF
E11A	GLFDIIKKIAASF
S12A	GLFDIIKKIAEAF
F13A	GLFDIIKKIAESA
K7H	GLFDIIHKIAESF
K8H	GLFDIIKHIAESF
E11H	GLFDIIKKIAHSF
K7R	GLFDIIKRKIAESF
K8R	GLFDIIKRKIAESF
E11R	GLFDIIKKIARSF
E11D	GLFDIIKKIADSF

^aAn alanine scan was performed on aurein 1.2 to determine positions that tolerate mutation. Charged amino acids at tolerant positions were then replaced with histidines or other charged amino acids in an attempt to increase endosomal escape efficiency. All constructs were expressed as recombinant fusion proteins with +36 GFP–Cre.

alanine substitution. Six positions retained >70% of the activity of unmutated aurein 1.2–+36 GFP–Cre (Figure 4A). At each of these tolerant positions, which included three positions with charged residues (K7, K8, and E11 from Table 2), we generated additional mutations in an effort to improve activity. In total, 19 mutants of aurein 1.2 were generated and tested using the Cre recombination assay. Two of the aurein variants, K8R and S12A, exhibited potentially improved overall recombination efficiency but also increased toxicity at 250 nM (Figure 4B). Given this increase in toxicity, we decided to focus on the original peptide, aurein 1.2, and proceeded to characterize its potency through a series of complementary secondary assays.

Independent Assays of Endosomal Escape. Although endosomal escape is widely considered to be the major bottleneck of cationic protein delivery,³⁴ few assays quantify the ability of proteins to escape endosomes on a single-cell basis. To quantify cytosolic delivery of supercharged proteins in individual cells, we applied a glucocorticoid receptor (GR) translocation assay³⁵ described by Schepartz and colleagues.^{9,36}

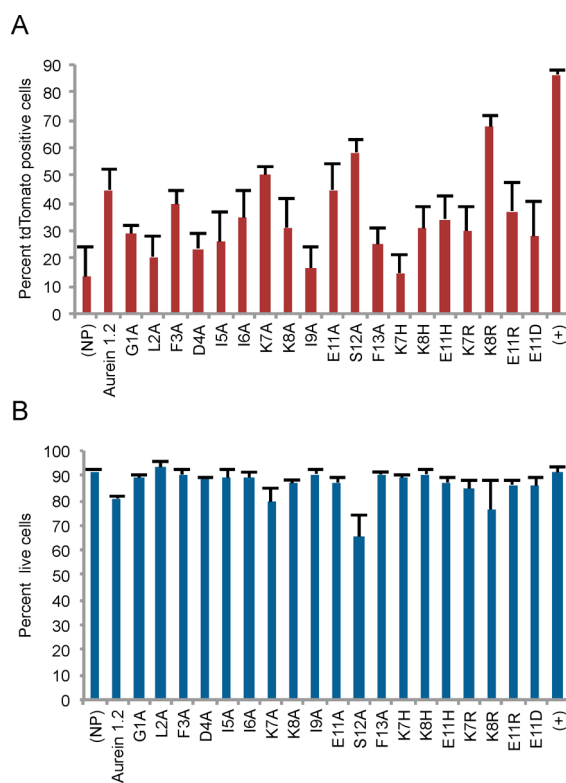


Figure 4. Activity and cytotoxicity of aurein 1.2 variants fused to +36 GFP–Cre (A) The percentage of tdTomato positive cells was determined by flow cytometry. (B) Toxicity as determined by CellTiterGlo (Promega) assay. For (A) and (B), 250 nM +36 GFP–Cre was used as the no peptide control (NP), and addition of 100 μ M chloroquine was used as the positive control (+). Cells were treated with 250 nM protein for 4 h in serum-free DMEM. Cells were washed and supplemented with full DMEM and incubated for 48 h.

In untreated HeLa cells expressing mCherry-labeled GR (GR-mCherry), the GR distributes nearly uniformly throughout the cell interior, resulting in a nuclear-to-cytoplasm translocation ratio (TR) of 1.17 (Figure 5A and 5B). Upon treatment with the cell-permeable glucocorticoid dexamethasone-21-thiopropionic acid (SDex) at a concentration of 1 μ M for 30 min, GR-mCherry relocates almost exclusively to the nucleus, resulting in a TR of 3.77 (Figure 5A and 5B).

We generated dexamethasone conjugates of +36 GFP (+36 GFP^{Dex}) and aurein 1.2–+36 GFP (aurein 1.2–+36 GFP^{Dex}) via sortase-mediated conjugation (Supporting Information Figure S4). Conjugated to these proteins, SDex is no longer cell permeable and cannot activate the GR for nuclear translocation unless the protein-SDex conjugate can access the cytosol. Treatment of HeLa cells expressing GR-mCherry with 1 μ M aurein 1.2–+36 GFP^{Dex} for 30 min resulted in a TR of 2.62, which was significantly greater ($p < 0.05$) than that of +36 GFP^{Dex} (TR = 2.23). As positive controls, we treated these cells with canonical cell permeable peptides (Tat^{Dex} and Arg^{8Dex}) and miniature proteins containing a penta-arg that reach the cytosol intact, with efficiencies exceeding 50% (5.3^{Dex} and ZF 5.3^{Dex}).³⁷ Aurein 1.2–+36 GFP^{Dex} (TR = 2.62), activated significantly greater levels of GR-mCherry translocation ($p < 0.001$) than Tat^{Dex} (TR = 1.87) and Arg^{8Dex} (TR = 1.63) and similar levels evoked by miniature proteins 5.3^{Dex} (TR = 2.62) and ZF 5.3^{Dex} (TR = 2.38) (Figure 5A and 5B). Taken together, these results suggest that aurein 1.2–+36

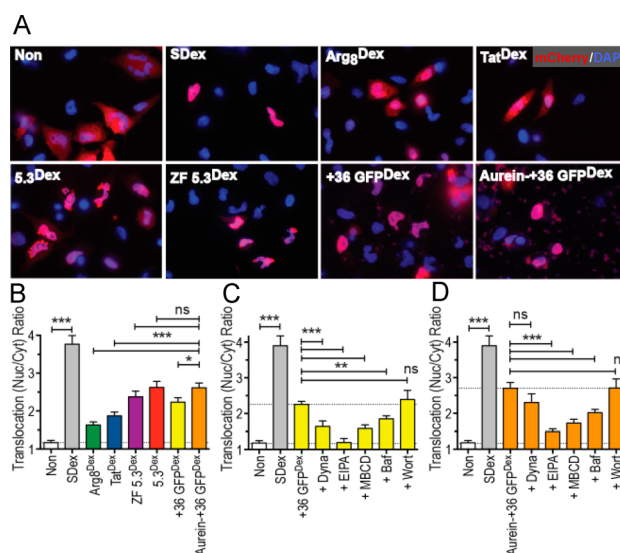


Figure 5. Investigating the ability of +36 GFP and aurein 1.2–+36 GFP dexamethasone-conjugates to reach the cytosol and activate GR translocation. (A) Images of HeLa cells expressing GR-mCherry treated in the presence and absence of 1 μ M dexamethasone (Dex)-protein conjugates for 30 min at 37 $^{\circ}$ C. (B) Nuclear-to-cytoplasm GR-mCherry fluorescence ratios (translocation ratios) of respective Dex-protein conjugates determined using CellProfiler. (C) GR-mCherry translocation ratios resulting from cells treated in the presence and absence of +36 GFP^{Dex} and endocytic inhibitors. (D) GR-mCherry translocation ratios resulting from cells treated in the presence and absence of aurein 1.2–+36 GFP^{Dex} and endocytic inhibitors. Statistical significance is measured by P -value. ns = $P > 0.05$, * = $P \leq 0.05$, ** = $P \leq 0.01$, *** = $P \leq 0.001$.

GFP^{Dex} exhibits an improved ability to access the cytoplasm over +36 GFP^{Dex} and canonical cell permeable peptides.

As an additional, independent assay of nonendosomal protein delivery, we tested the ability of aurein 1.2 to enhance the nonendosomal delivery of an evolved biotin ligase (BirA) enzyme developed by Ting and co-workers.³⁸ BirA catalyzes the biotinylation of a 15-amino acid acceptor peptide (AP). We transfected mCherry-AP fusion plasmid into HeLa cells. Biotinylation of mCherry can only occur in the presence of cytosolic BirA. To assess the nonendosomal delivery of +36 GFP–BirA protein, mCherry-AP biotinylation was quantified by Western blot using fluorophore-labeled streptavidin and normalized to the mCherry signal (Supporting Information Figure S5A). Treatment with 250 nM aurein 1.2–+36 GFP–BirA resulted in a 50% increase in biotinylation signal compared with 250 nM of +36 GFP–BirA alone (Supporting Information Figure S5B). We also observed a dose-dependent increase in AP-biotinylation across treatment concentrations (250 nM, 500 nM, and 1 μ M) for both aurein 1.2–(+36 GFP)–BirA and unfused +36 GFP–BirA constructs. These results are consistent with the results of the GR translocation assay, and further suggest that aurein 1.2 enhances the endosomal escape of superpositively charged proteins.

In order to directly quantify the increase in nonendosomal delivery resulting from aurein 1.2, we performed a cytosolic fractionation experiment to calculate the cytosolic concentrations of delivered protein. HeLa cells were treated with +36 GFP or aurein 1.2–+36 GFP at 250 nM, 500 nM, and 1 μ M. After 30 min of treatment, cells were washed, homogenized, and fractionated by ultracentrifugation. The cytosolic concentration of delivered protein was calculated from the GFP

fluorescence of the cytosolic fraction together with a standard curve relating fluorescence to known concentrations of +36 GFP and aurein 1.2+36 GFP added to cytosolic extract (Supporting Information Figures S6B and S6C). At 250 nM, treatment with aurein 1.2+36 GFP resulted in ~5-fold more delivered cytosolic protein than treatment with +36 GFP alone (Supporting Information Figure S6A). This difference decreased with increasing protein concentration, likely due to the influence of alternate uptake pathways or delivery bottlenecks at high protein concentrations. In contrast, the total amount of aurein 1.2+36 GFP versus +36 GFP uptaken by cells was similar, with aurein 1.2+36 GFP showing 1.3-fold higher total cellular uptake at 250 nM. These results directly demonstrate that aurein 1.2 increases the cytosolic concentration of cationic proteins that enter cells predominantly through endosomes,^{14,18} and are consistent with the above findings that aurein 1.2 has the greatest effect on enhancing nonendosomal delivery at ~250 nM (Figure 3A).

Effect of Endocytic Inhibitors on +36 GFP and Aurein 1.2+36 GFP Delivery. We previously reported that endocytosis plays a key role in the cytosolic delivery of superpositively charged proteins.¹⁸ To probe the role of endocytosis in the delivery of supercharged proteins with or without aurein 1.2, we treated cells expressing GR-mCherry with either +36 GFP^{Dex} or aurein 1.2+36 GFP^{Dex} in the presence of known endocytic inhibitors. The cortical actin remodeling inhibitor *N*-ethyl-isopropyl amiloride (EIPA), the cholesterol-sequestering agent methyl- β -cyclodextrin (MBCD), and the endosomal vesicular ATPase inhibitor bafilomycin (Baf) all strongly reduced the ability of both proteins to stimulate GR-mCherry translocation. Blocking maturation of Rab5⁺ vesicles by treatment with the phosphatidylinositol 3-kinase inhibitor wortmannin (Wort) did not influence reporter translocation of either +36 GFP^{Dex} or aurein 1.2+36 GFP^{Dex} (Figure 5C and 5D). In contrast, treatment with the small-molecule dynamin II inhibitor Dynasore (Dyna) significantly suppressed the ability of +36 GFP^{Dex} to stimulate GR-mCherry translocation (TR = 1.64) (Figure 5C) but had little influence on the cytosolic delivery of aurein 1.2+36 GFP^{Dex} (TR = 2.30) (Figure 5D). Taken together, these results suggest that active endocytosis is required for uptake of +36 GFP and aurein 1.2+36 GFP into the cell interior, and that the two proteins may traffic differently into the cell interior.

Aurein 1.2 Can Greatly Increase Protein Delivery Efficiency in Vivo. To evaluate the ability of aurein 1.2 to increase the efficacy of cationic protein delivery in vivo, we delivered proteins to the inner ear of Cre reporter transgenic mice that express tdTomato upon Cre-mediated recombination. This animal model was chosen due to its confined injection volume, the presence of well-characterized cell types, and the existence of genetic deafness models that would facilitate future studies of protein delivery to treat hearing loss. We previously showed that +36 GFP-Cre alone can be delivered to mouse retina,¹⁵ albeit resulting in only modest levels of recombination consistent with inefficient endosomal escape.

Anesthetized postnatal day 2 (P2) mice were injected with 0.4 μ L of 50 μ M +36 GFP-Cre or aurein 1.2+36 GFP-Cre solutions in the scala media to access the cochlear cells. Five days after injection, the cochleas were harvested for immunolabeling of inner ear cell markers and imaging for tdTomato fluorescence (Figure 6A). We evaluated both the hair cells (Myo7a+) and supporting cells (Myo7a-) for tdTomato

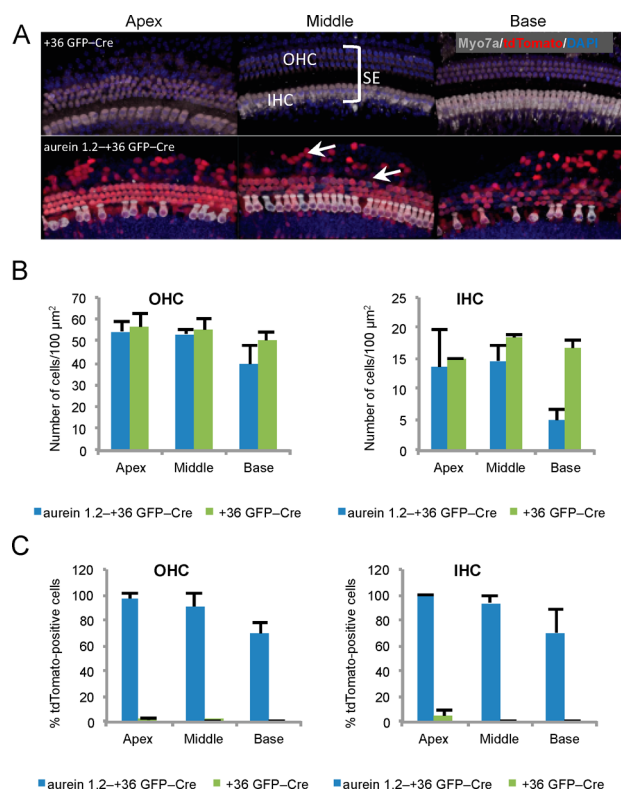


Figure 6. In vivo protein delivery of Cre recombinase into mouse neonatal cochleas. 0.4 μ L of 50 μ M +36 GFP-Cre or aurein 1.2+36 GFP-Cre were injected into the scala media. (A) Five days after injection, cochlea were harvested. Inner hair cells (IHC), outer hair cells (OHC) and supporting cells in the sensory epithelium (SE) were imaged for the presence of tdTomato, which is only expressed following Cre-mediated recombination. Hair cells were labeled with antibodies against the hair-cell marker Myo7a. Gray/white = Myo7a, Red = tdTomato, Blue = DAPI. (B) To evaluate cytotoxicity, the number of outer hair cells and inner hair cells were measured by counting DAPI-stained cells (C) The percentage of tdTomato positive cells, reflecting successful delivery of functional Cre recombinase, was determined by fluorescence imaging.

signal. The total number of hair cells and supporting cells (by DAPI labeling) in the sensory epithelium (SE) was used to determine the relative toxicity of aurein 1.2+36 GFP-Cre to the baseline treatment of +36 GFP-Cre (Figure 6A). Overall, an average of 96%, 92% and 66% of cochlear cells survived aurein 1.2+36 GFP-Cre treatment as compared to +36 GFP-Cre treatment in the apex, middle, and base tissue samples, respectively (Figure 6A). +36 GFP-Cre treatment resulted in low levels of recombination only in inner hair cells (IHC) of the apex of the cochlea (4.4%) but not in the middle or base of the cochlear hair cells or any cochlear supporting cells. In contrast, treatment with aurein 1.2+36 GFP-Cre resulted in very high Cre-mediated recombination levels throughout the apex, middle, and base samples of outer hair cells (OHC) (96%, 92%, and 66%, respectively), inner hair cells (100%, 94%, and 70%, respectively), as well as supporting cells (arrows) (Figure 6A and 6C).

The observed levels of recombination in the inner hair cells from aurein 1.2+36 GFP-Cre are comparable to that of adeno-associated virus type 1 (AAV1) gene transfection.³⁹ For outer hair cells, we have previously shown similar levels of recombination using liposome-mediated delivery of super-negatively charged GFP-Cre.⁴⁰ The aurein 1.2+36 GFP-Cre

delivery system is the only method that showed significant recombination levels in both inner and outer hair cells,^{39,41} and does not require any virus or other molecules beyond a single polypeptide. Significantly, aurein 1.2-+36 GFP-Cre also extended delivered recombinase activity to additional cochlear supporting cells. These results suggest aurein 1.2-+36 GFP-Cre delivery system to be a promising method for in vivo protein delivery into both hair cells and supporting cells of the inner ear.⁴²

CONCLUSION

We discovered a 13-residue peptide, aurein 1.2, that can increase the efficiency of nonendosomal protein delivery by screening a panel of known membrane-active peptides. The results from a small screen of 22 peptides are consistent with our hypothesis that some peptides can selectively disrupt the endosomal membrane without disrupting the mammalian cell membrane. The effectiveness of aurein 1.2 is highly dependent on its sequence, as several other closely related peptides did not enhance protein delivery (Tables 1 and 2). Subtle differences in amino acid composition led to dramatic changes in membrane activity among peptides tested, highlighting the difficulty of rationally designing peptides that enhance nonendosomal delivery. Moreover, the lack of correspondence between peptide cationic charge and nonendosomal delivery efficiency suggests that aurein 1.2 does not enhance nonendosomal delivery simply by promoting endocytosis. While none of the tested variants of aurein 1.2 substantially outperformed the original peptide, we identified several amino acids that could be altered without loss of activity. These findings also provide a starting point for further optimization to discover next-generation endosomolytic peptides with improved efficacy and reduced toxicity.

Four independent assays for nonendosomal protein delivery (Cre recombination, GR translocation, BirA activity on a cytoplasmic peptide, and cytosolic fractionation), together with the peptide mutational studies described above, collectively suggest that aurein 1.2-fusion enhances endosomal escape of superpositively charged proteins. Moreover, these assays collectively demonstrate the ability of aurein 1.2 to mediate the nonendosomal delivery of +36 GFP fused to different proteins (or small molecules), suggesting that aurein 1.2 facilitates endosomal escape in a manner that is at least somewhat cargo-independent.

The in vivo protein delivery experiments described above revealed dramatic increases in nonendosomal functional Cre recombinase delivery into the diverse inner ear cell types including hair cells and supporting cells of live mice upon fusion with aurein 1.2. Indeed, aurein 1.2-fused +36 GFP-Cre construct resulted in highly efficient recombination levels across the main cochlear sensory epithelial cell classes studied in this work, all but one of which were unaffected by +36 GFP-Cre treatment. Taken together, these results suggest that aurein 1.2 is a 13-residue, potent, genetically encodable, endosome escape-enhancing peptide that can greatly increase the efficiency of nonendosomal cationic protein delivery in vitro and in vivo without requiring the use of additional components beyond the protein of interest.

EXPERIMENTAL SECTION

Construction of Expression Plasmids. Sequences of all constructs used in this paper are listed in the Supporting Information. All protein constructs were generated from previously reported

plasmids for protein of interest cloned into a pET29a expression plasmid.⁴³ All plasmid constructs generated in this work will be deposited with Addgene.

Expression and Purification of Proteins. *E. coli* BL21 STAR (DE3) competent cells (Life Technologies) were transformed with pET29a expression plasmids. Colonies from the resulting expression strain was directly inoculated in 1 L of Luria-Bertani (LB) broth containing 100 $\mu\text{g}/\text{mL}$ of ampicillin at 37 °C to $\text{OD}_{600} = \sim 1.0$. Isopropyl β -D-1-thiogalactopyranoside (IPTG) was added at 0.5 mM to induce expression and the culture was moved to 20 °C. After ~ 16 h, the cells were collected by centrifugation at 6000g and resuspended in lysis buffer (phosphate buffered saline (PBS) with 1 M NaCl). The cells were lysed by sonication (1 s pulse-on, 1 s pulse-off for 6 min, twice, at 6 W output) and the soluble lysate was obtained by centrifugation at 10 000g for 30 min.

The cell lysate was incubated with His-Pur nickel-nitriloacetic acid (Ni-NTA) resin (Thermo Scientific) at 4 °C for 45 min to capture His-tagged protein. The resin was transferred to a 20 mL column and washed with 20 column volumes of lysis buffer plus 50 mM imidazole. Protein was eluted in lysis buffer with 500 mM imidazole, and concentrated by Amicon ultra centrifugal filter (Millipore, 30-kDa molecular weight cutoff) to ~ 50 mg/mL. The eluent was injected into a 1 mL HiTrap SP HP column (GE Healthcare) after dilution into PBS (5-fold). Protein was eluted with PBS containing a linear NaCl gradient from 0.1 to 1 M over five column volumes. The eluted fractions containing protein were concentrated to 50 μM as quantified by absorbance at 488 nm assuming an extinction coefficient of $8.33 \times 10^4 \text{ M}^{-1} \text{ cm}^{-1}$ as previously determined,¹⁴ snap-frozen in liquid nitrogen, and stored in aliquots at -80 °C.

Cell Culture. All cells were cultured in Dulbecco's modification of Eagle's medium (DMEM w/glutamine, Gibco) with 10% fetal bovine serum (FBS, Gibco), 5 IU penicillin, and 5 g/mL streptomycin. All cells were cultured at 37 °C with 5% CO_2 .

Peptide Synthesis. Peptides were ordered from ChinaPeptides Co., LTD, each 4 mg, purity >90%. HPLC and MALDI data were provided with lyophilized peptides. Peptides were resuspended in DMSO to a final concentration of 10 mM.

Sortase Conjugation. All reactions were performed in 100 mM Tris buffer (pH 7.5) with 5 mM CaCl_2 and 1 M NaCl. For peptide conjugation to the N-terminus of GGG-+36-GFP, 20 μM of protein with N-terminal Gly-Gly-Gly was incubated with 400 μM of peptide with C-terminal LPETGG and 1 μM eSrtA for 2 h at room temperature in a 50 μL reaction. The unreacted peptides were removed through spin filtration with an Amicon Ultra-0.5 Centrifugal Filter Unit (Millipore, 30-kDa molecular weight cutoff). The reaction mixture was washed twice with 500 μL of buffer each time to a volume of 50 μL . Conjugation efficiency was determined through LC-MS (Agilent 6220 ESI-TOF) using protein deconvolution through MaxEnt (Waters) by comparing relative peak intensities.

For conjugation of GGGK^{Dex} to +36-GFP-LPETG-His₆, 10 μM of protein was incubated with 400 μM of peptide and 2 μM eSrtA at room temperature. The reaction was quenched with 10 mM ethylenediaminetetraacetic acid (EDTA) after 2 h. For aurein 1.2-+36-GFP-LPETG-His₆, an N-terminal His₆-ENLYFQ was added to prevent sortase reaction with the N-terminal glycine of aurein 1.2. The N-terminal tag was removed with 200 μM TEV protease at 4 °C for 16 h to release the native N-terminal sequence of aurein 1.2-+36-GFP. Successful conjugation of GGGK^{Dex} removes the C-terminal His₆ tag and allows for purification through reverse Ni-NTA column. Unreacted protein binds to the Ni-NTA, and the unbound protein was collected and concentrated as described above.

Plasmid Transfection. Plasmid DNA was transfected using Lipofectamine 2000 (Life Technologies) according the manufacturer's protocol.

Synthesis of Dexamethasone-21 Thiopropionic Acid (SDex). Synthesis of dexamethasone-21-mesylate was performed as previously described.^{44,45} 2 g of dexamethasone stirring in 38 mL anhydrous pyridine under nitrogen was reacted with 467.2 mg methanesulfonyl chloride (1.2 equiv) on ice for 1 h, after which another 311 mg methanesulfonylchloride was added and allowed to

react overnight (16 h) on ice. Next, the reaction was added to 800 mL of ice water and dexamethasone-21-mesylate (Dex-21-OMs) formed a white precipitate. The slurry was filtered and the precipitate washed with 800 mL of ice water, dried under high vacuum overnight and quantified by LC-MS (m/z 471.19 Da, 83% yield).

Dexamethasone-21-thiopropionic acid (SDex) was prepared as previously described.⁴⁶ 2.05 g of Dex-21-OMs was added to 2 equiv thiopropionic acid and 4 equiv triethylamine stirring in anhydrous acetone at room temperature overnight. The following morning, the reaction was added to 800 mL of ice water and acidified with 1 N HCl until SDex, visible as an off-white solid, precipitation was complete. The mixture was filtered, washed with 800 mL ice cold water acidified to pH 1 with HCl, dried under high vacuum overnight and analyzed by LC-MS (m/z 481.21 Da, 63% yield) (Supporting Figure S7).

Synthesis and Purification of GGGK^{Dex}. GGGK^{Dex} was synthesized on Fmoc-Lys (Mtt)-Wang resin (BACHEM, D-2565) using microwave acceleration (MARS, CEM). Coupling reactions were performed using 5 equiv of Fmoc-Gly-OH (Novabiochem, 29022–11–5), 5 equiv of PyClock (Novabiochem, 893413–42–8) and 10 equiv of diisopropylethylamine (DIEA) in *N*-methylpyrrolidone (NMP). Fmoc groups were removed using 25% piperidine in NMP (efficiency quantified; $\epsilon_{299} = 6234 \text{ M}^{-1} \text{ cm}^{-1}$ in acetonitrile) and Mtt groups were removed by incubating the Fmoc-GGGK(Mtt)-resin with 2% trifluoroacetic acid (TFA) in dichloromethane (DCM) for 20 min, after which the resin was washed with 2% TFA in DCM until the characteristic yellow color emitting from the Mtt cation subsided. After Mtt removal, SDex-COOH (Dex-21-thiopropionic acid³⁵) was coupled to the N ϵ of the lysine side-chain by incubating the Fmoc-GGGK-resin with 2.5 equiv SDex-COOH, 2.5 equiv HATU, 2.5 equiv HOAt, 5 equiv DIEA and 5 equiv 2,6-lutidine in 2.5 mL NMP overnight, at room temperature, on an orbital shaker. After SDex-labeling, Fmoc-GGGK^{Dex}-resin was washed thoroughly with NMP and DCM, the N-terminal Fmoc was removed using 25% piperidine in NMP, and crude peptides were dissociated from the resin by incubating the GGGK^{Dex}-resin in a cleavage cocktail composed of 81.5% trifluoroacetic acid (TFA), 5% thioanisole, 5% phenol, 5% water, 2.5% ethanedithiol and 1% triisopropylsilane for 30 min at 38 °C. Crude peptides were precipitated in 40 mL cold diethyl ether, resuspended in water, lyophilized and purified via reverse phase high-pressure liquid chromatography (HPLC) using a linear gradient of acetonitrile and water with 0.1% TFA across a C18 (VYDAC, 250 mm \times 10 mm ID) column. Purified peptides were lyophilized and stored at 4 °C. Polypeptide identity was confirmed by mass spectrometry on a Waters QToF LC-MS, and purity was measured by analytical reverse-phase HPLC (Shimadzu Instruments) using a C18 column (Poroshell 120 SB-C18, 2.7 μm , 100 mm \times 3 mm ID, Agilent).

Image Processing for Primary Screen. BSRLNL.tdTomato cells were plated at 10 000 cells per well in black 384-well plates (Aurora Biotechnologies). Cells were treated with Cre fusion proteins diluted in serum-free DMEM 24 h after plating and incubated for 4 h at 37 °C. Following incubation, the cells were washed three times with PBS + 20 U/mL heparin. The cells were incubated a further 48 h in serum-containing media. Cells were fixed in 3% paraformaldehyde and stained with Hoechst 33342 nuclear dye. Images were acquired on an ImageXpress Micro automated microscope (Molecular Devices) using a 4 \times objective (binning 2, gain 2), with laser- and image-based focusing (offset $-130 \mu\text{m}$, range $\pm 50 \mu\text{m}$, step $25 \mu\text{m}$). Images were exposed for 10 ms in the DAPI channel (Hoechst) and 500 ms in the dsRed channel (tdTomato). Image analysis was performed using the cell-scoring module of MetaXpress software (Molecular Devices). All nuclei were detected with a minimum width of 1 pixel, maximum width of 3 pixels, and an intensity of 200 gray levels above background. Positive cells were evaluated for uniform signal in the dsRed channel (minimum width of 5 pixels, maximum width of 30 pixels, intensity >200 gray levels above background, $10 \mu\text{m}$ minimum stained area). In total, nine images were captured and analyzed per well, and 16 wells were treated with the same fusion protein. The primary screen was completed in biological triplicate.

Cre Delivery Assay. Uptake and delivery assays for Cre fusion proteins were performed as previously described.¹⁵ Briefly, proteins

were diluted in serum-free DMEM and incubated on the cells in 48-well plates for 4 h at 37 °C. Following incubation, the cells were washed three times with PBS + 20 U/mL heparin. The cells were incubated a further 48 h in serum-containing media prior to trypsinization and analysis by flow cytometry. All flow cytometry were carried out on a BD Fortessa flow cytometer (Becton-Dickinson) using 530/30 nm and 610/20 nm filter sets. Toxicity for aurein 1.2 and citropin 1.3 validation assays was determined using CellTiterGlo assay (Promega) in 96-well plates following manufacturer protocol. Toxicity for alanine scan mutational analysis was determined with LIVE/DEAD fixable far-red dead cell stain (Life Technologies) with 635 nm laser and 670/30 nm filter.

GR-mCherry Translocation Assay. One day prior to transfection 10 000 HeLa cells in 200 μL of DMEM (10% FBS, 1 \times PenStrep) were plated into single wells of a 96-well MatriCal glass bottom microplate (MGB096-1-2-LG-L) and allowed to adhere overnight. The following day, cells were transfected with GR-mCherry⁹ using Lipofectamine 2000 technologies. Following transfection, cells were allowed to recover overnight in DMEM (+ 10% FBS). The following day, cells were treated with dexamethasone (Dex) or 1 μM Dex-protein conjugate in the presence or absence of inhibitor diluted into DMEM (without phenol red, + 300 nM Hoechst33342). After 30 min, cells were washed twice with 200 μL of HEPES–Krebs–Ringer's (HKR) buffer (140 mM NaCl, 2 mM KCl, 1 mM CaCl₂, 1 mM MgCl₂, and 10 mM HEPES at pH 7.4), after which 100 μL of HKR buffer was overlaid onto the cells and images were acquired on a Zeiss Axiovert 200 M epifluorescence microscope outfitted with Zeiss AxioCamRM camera and an EXFO-Excite series 120 Hg arc lamp. The translocation ratio (the ratio of median GFP intensity in the nuclear and surrounding regions) for individual cells was measured using CellProfiler as described.³⁶ To examine the effect of endocytosis inhibitors, HeLa cells were pretreated for 30 min with DMEM (without phenol red) containing inhibitors (80 μM Dynasore, 5 mM MBCD, 50 μM EIPA, 200 nM bafilomycin or 200 nM wortmannin) at 37 °C before incubation with Dex or Dex-protein conjugates.

BirA Translocation Assay. One day prior to transfection, 100 000 HeLa cells in 1 mL of DMEM (10% FBS, 1 \times PenStrep) were plated into single wells of a 12-well tissue culture plate and allowed to adhere overnight. Cells were transfected with mCherry-AP fusion protein using Lipofectamine 2000 technologies according to manufacture guidelines 24 h before protein treatment. Next day, transfected cells were treated for 1 h at 37 °C with +36 GFP–BirA or aurein 1.2–+36 GFP–BirA diluted in serum-free DMEM at 250 nM, 500 nM and 1 μM concentrations. 250 nM + 36 GFP–BirA + 100 μM chloroquine was also used as a positive control for endosomal escape. The cells were washed three times with PBS containing heparin to remove excess supercharged proteins that were not internalized. The cells were then treated with 100 μL of 10 μM biotin and 1 mM ATP in PBS for 10 min. The reaction was quenched with excess (10 μL of 8 mM) synthesized AP before cells were trypsinized and lysed. To verify that extracellular BirA was not generating signal during lysis, 1 μM + 36 GFP–BirA or aurein 1.2–+36 GFP–BirA was added during the quench step to untreated wells. Cells were lysed with 100 μL of trypsin and lysed with QIAshredder columns (Qiagen). Thirty μL of lysate was loaded onto 4–12% Bis-Tris Bolt gels in Bolt-MES buffer (Life Technologies) and ran for 20 min at 200 V. Gels were transferred to PVDF membrane using iBlot2 transfer system (Life Technologies). Biotinylation was measured through Western blotting using the LI-COR quantitative infrared fluorescent antibodies and the Odyssey Imager detection system. To normalize for transfection and gel loading variability, the ratio of biotin signal to mCherry signal was used for comparison.

Cytosolic Fractionation Assay. One day prior to fractionation, 4 \times 10⁶ HeLa cells were plated in 20 mL of DMEM (10% FBS, 1 \times PenStrep, no phenol red) in 175 cm² culture flasks and allowed to adhere for 15 h. The following day, the media was removed from each flask and the cells were washed twice with clear DMEM (no FBS, no PenStrep, no phenol red). The media was replaced with 7 mL of clear DMEM containing +36 GFP or aurein 1.2–+36 GFP at a concentration of 250 nM, 500 nM, or 1 μM . Several flasks were

treated with clear DMEM to be used as negative controls and to generate calibration curves with the cytosolic extracts. The cells were incubated for 30 min at 37 °C, 5% CO₂ after which they were washed three times with PBS. Using a cell-scraper, the cells were suspended in 5 mL of PBS, transferred into a 15 mL Falcon tube, and pelleted at 500g for 3 min. The cells were resuspended in 1 mL PBS, counted using an automated cell counter (Auto T4, Cellometer), and pelleted again at 500g for 3 min. The cell pellet was resuspended in ice-cold isotonic sucrose (290 mM sucrose, 10 mM imidazole, pH 7.0 with 1 mM DTT, and cOmplete, EDTA-free protease inhibitor cocktail) and transferred to a glass test tube on ice. The cells were homogenized with an Omni TH homogenizer outfitted with a stainless steel 5 mm probe for three 30 s pulses on ice with 30 s pauses between the pulses. The homogenized cell lysate was sedimented at 350 Kg in an ultracentrifuge (TL-100; Beckman Coulter) for 30 min at 4 °C using a TLA 120.2 rotor. The supernatant (cytosolic fraction) was analyzed in a black clear bottom 96-well plate on a fluorescence plate reader (Synergy 2, BioTek, excitation = 485 ± 10 nm, emission = 528 ± 10 nm). The concentration of the protein conjugate in the cytosol was determined using a standard curve relating fluorescence to known protein concentrations. To generate the standard curve, known concentrations of +36 GFP and aurein 1.2-+36 GFP between 0.2 nM and 1 μM were added to cytosolic extracts of the untreated negative controls. For background subtraction, several wells containing cytosolic extracts from untreated cells were averaged, and this average was subtracted from each well.

Total Protein Delivery Assay. One day prior to the experiment, 100 000 HeLa cells/well were plated in DMEM (10% FBS, 1× PenStrep, no phenol red) in 6-well plates and allowed to adhere for 15 h. The following day, the media was removed from each well and the cells were washed twice with clear DMEM (no FBS, no PenStrep, no phenol red). The media was replaced with 1 mL of clear DMEM containing +36 GFP or aurein 1.2-+36 GFP at concentrations of 250 nM, 500 nM, or 1 μM. The cells were incubated for 30 min at 37 °C, 5% CO₂ after which they were washed three times with PBS containing 20 U/mL heparin (Sigma) to remove surface-bound cationic protein. The cells were trypsinized for 5 min, pelleted in serum-containing DMEM for 3 min at 500g, washed with 1 mL PBS, and pelleted again for 3 min at 500g. The cell pellet was resuspended in 100 μL PBS. Flow cytometry was performed on a BD Accuri C6 Flow Cytometer at 25 °C. Cells were analyzed in PBS (excitation laser = 488 nm, emission filter = 533 ± 30 nm). At least 10 000 cells were analyzed for each sample. For background subtraction, wells were treated with clear DMEM only. The average of three untreated wells was subtracted from each +36 GFP conjugate-containing well.

Microinjection of Proteins to Mouse Inner Ear. P1-2 Gt(ROSA)26Sor^{tm14(CAG-tdTomato)Hze} mice were used for aurein 1.2-+36-GFP-Cre and +36-GFP-Cre injection. The Rosa26-tdTomato mice were from the Jackson Laboratory. Animals were used under protocols approved by the Massachusetts Eye and Ear Infirmary IACUC committee. Mice were anesthetized by hypothermia on ice. Cochleostomies were performed by making an incision behind the ear to expose the cochlea. Glass micropipettes held by a micromanipulator were used to deliver the complex into the scala media, which allows access to inner ear hair cells. The total delivery volume for every injection was 0.4 μL per cochlea and the release was controlled by a micromanipulator at the speed of 69 nL/min.

Immunohistochemistry and Quantification. Five days after injection, the mice were sacrificed and cochlea were harvested by standard protocols.⁴⁷ For immunohistochemistry, antibodies against hair-cell markers (Myo7a) and supporting cells (Sox2) were used following a previously described protocol.⁴⁷ To quantify the number of tdTomato positive cells after aurein 1.2-+36-GFP-Cre and +36-GFP-Cre, we counted the total number of inner and outer hair cells in a region spanning 100 μm in the apex, middle, and base turn of the cochlea.

■ ASSOCIATED CONTENT

📄 Supporting Information

The Supporting Information is available free of charge on the ACS Publications website at DOI: 10.1021/jacs.5b05694.

Additional information and experimental methods. List of all protein constructs included. (PDF)

■ AUTHOR INFORMATION

Corresponding Author

*drlu@fas.harvard.edu

Notes

The authors declare the following competing financial interest(s): DRL is a founder of Permeon Biologics, a company that uses supercharged proteins for therapeutic purposes..

■ ACKNOWLEDGMENTS

This work was supported by the Howard Hughes Medical Institute and the NIH/NIGMS (R01 GM095501) the NIH/NIDCD (R01 DC006908). M.L. was supported by fellowships from Harvard CCB. Y.T. and Y.S were supported by the Frederick and Ines Yeatts Hair Cell Regeneration grant. Y.S. was supported by The National Nature Science Foundation of China (NSFC81300824). Angela Steinauer is a Howard Hughes Medical Institute International Student Research fellow. We are grateful to Thomas Hasaka and Nicola Tolliday of the Broad Institute for assistance with the primary screen.

■ REFERENCES

- (1) Nelson, A. L.; Dhimolea, E.; Reichert, J. M. *Nat. Rev. Drug Discovery* **2010**, *9*, 767.
- (2) Huang, C. *Curr. Opin. Biotechnol.* **2009**, *20*, 692.
- (3) Hafler, D. A. *Nat. Rev. Immunol.* **2007**, *7*, 423.
- (4) Leader, B.; Baca, Q. J.; Golan, D. E. *Nat. Rev. Drug Discovery* **2008**, *7*, 21.
- (5) Schiffmann, R.; Kopp, J. B.; Austin, H. A.; Sabins, S.; Moore, D. R.; Weibel, T.; Balow, J. E.; Brady, R. O. *JAMA* **2001**, *285*, 2743.
- (6) Spiegelman, B. M. *Diabetes* **1998**, *47*, 507.
- (7) Mali, P.; Esvelt, K. M.; Church, G. M. *Nat. Methods* **2013**, *10*, 957.
- (8) Mueller, J.; Kretzschmar, I.; Volkmer, R.; Boisguerin, P. *Bioconjugate Chem.* **2008**, *19*, 2363.
- (9) Appelbaum, J. S.; LaRochelle; Jonathan, R.; Smith, B. A.; Balkin; Daniel, M.; Holub, J. M.; Schepartz, A. *Chem. Biol.* **2012**, *19*, 819.
- (10) Rizk, S. S.; Luchniak, A.; Uysal, S.; Brawley, C. M.; Rock, R. S.; Kosiakoff, A. A. *Proc. Natl. Acad. Sci. U. S. A.* **2009**, *106*, 11011.
- (11) Hasadsri, L.; Kreuter, J.; Hattori, H.; Iwasaki, T.; George, J. M. *J. Biol. Chem.* **2009**, *284*, 6972.
- (12) Fu, A.; Tang, R.; Hardie, J.; Farkas, M. E.; Rotello, V. M. *Bioconjugate Chem.* **2014**, *25*, 1602.
- (13) Pisal, D. S.; Kosloski, M. P.; Balu-Iyer, S. V. *J. Pharm. Sci.* **2010**, *99*, 2557.
- (14) McNaughton, B. R.; Cronican, J. J.; Thompson, D. B.; Liu, D. R. *Proc. Natl. Acad. Sci. U. S. A.* **2009**, *106*, 6111.
- (15) Cronican, J. J.; Thompson, D. B.; Beier, K. T.; McNaughton, B. R.; Cepko, C. L.; Liu, D. R. *ACS Chem. Biol.* **2010**, *5*, 747.
- (16) Cronican, J. J.; Beier, Kevin, T.; Davis, Tina, N.; Tseng, J.-C.; Li, W.; Thompson, D. B.; Shih, A. F.; May, E. M.; Cepko, C. L.; Kung, A. L.; Zhou, Q.; Liu, D. R. *Chem. Biol.* **2011**, *18*, 833.
- (17) Lawrence, M. S.; Phillips, K. J.; Liu, D. R. *J. Am. Chem. Soc.* **2007**, *129*, 10110.
- (18) Thompson, D. B.; Villaseñor, R.; Dorr; Brent, M.; Zerial, M.; Liu; David, R. *Chem. Biol.* **2012**, *19*, 831.
- (19) Fuchs, S. M.; Raines, R. T. *ACS Chem. Biol.* **2007**, *2*, 167.
- (20) Pirie, C. M.; Hackel, B. J.; Rosenblum, M. G.; Wittrup, K. D. *J. Biol. Chem.* **2011**, *286*, 4165.

- (21) Varkouhi, A. K.; Scholte, M.; Storm, G.; Haisma, H. J. *J. Controlled Release* **2011**, *151*, 220.
- (22) Wadia, J. S.; Stan, R. V.; Dowdy, S. F. *Nat. Med.* **2004**, *10*, 310.
- (23) Neundorff, I.; Rennert, R.; Hoyer, J.; Schramm, F.; Löbner, K.; Kitanovic, I.; Wöfl, S. *Pharmaceuticals* **2009**, *2*, 49.
- (24) Sugita, T.; Yoshikawa, T.; Mukai, Y.; Yamanada, N.; Imai, S.; Nagano, K.; Yoshida, Y.; Shibata, H.; Yoshioka, Y.; Nakagawa, S. *Br. J. Pharmacol.* **2008**, *153*, 1143.
- (25) Zasloff, M. *Nature* **2002**, *415*, 389.
- (26) Lohner, K.; Blondelle, S. *Comb. Chem. High Throughput Screening* **2005**, *8*, 241.
- (27) Wang, Z.; Wang, G. *Nucleic Acids Res.* **2004**, *32*, D590.
- (28) Chen, I.; Dorr, B. M.; Liu, D. R. *Proc. Natl. Acad. Sci. U. S. A.* **2011**, *108*, 11399.
- (29) Dijkstra, J.; Van Galen, M.; Scherphof, G. L. *Biochim. Biophys. Acta, Mol. Cell Res.* **1984**, *804*, 58.
- (30) Rozek, T.; Bowie, J. H.; Wallace, J. C.; Tyler, M. J. *Rapid Commun. Mass Spectrom.* **2000**, *14*, 2002.
- (31) Wegener, K. L.; Wabnitz, P. A.; Carver, J. A.; Bowie, J. H.; Chia, B. C.; Wallace, J. C.; Tyler, M. J. *Eur. J. Biochem.* **1999**, *265*, 627.
- (32) Balla, M.; Bowie, J. H.; Separovic, F. *Eur. Biophys. J.* **2004**, *33*, 109.
- (33) Fernandez, D. I.; Le Brun, A. P.; Whitwell, T. C.; Sani, M.-A.; James, M.; Separovic, F. *Phys. Chem. Chem. Phys.* **2012**, *14*, 15739.
- (34) Sahay, G.; Querbés, W.; Alabi, C.; Eltoukhy, A.; Sarkar, S.; Zurenko, C.; Karagiannis, E.; Love, K.; Chen, D.; Zoncu, R. *Nat. Biotechnol.* **2013**, *31*, 653.
- (35) Yu, P.; Liu, B.; Kodadek, T. *Nat. Biotechnol.* **2005**, *23*, 746.
- (36) Holub, J. M.; LaRochelle, J. R.; Appelbaum, J. S.; Schepartz, A. *Biochemistry* **2013**, *52*, 9036.
- (37) LaRochelle, J. R.; Cobb, G. B.; Steinauer, A.; Rhoades, E.; Schepartz, A. *J. Am. Chem. Soc.* **2015**, *137*, 2536.
- (38) Howarth, M.; Ting, A. Y. *Nat. Protoc.* **2008**, *3*, 534.
- (39) Akil, O.; Seal, R. P.; Burke, K.; Wang, C.; Alemi, A.; Daring, M.; Edwards, Robert, H.; Lustig, L. R. *Neuron* **2012**, *75*, 283.
- (40) Zuris, J. A.; Thompson, D. B.; Shu, Y.; Guilinger, J. P.; Bessen, J. L.; Hu, J. H.; Maeder, M. L.; Joung, J. K.; Chen, Z.-Y.; Liu, D. R. *Nat. Biotechnol.* **2015**, *33*, 73.
- (41) Taura, A.; Taura, K.; Choung, Y. H.; Masuda, M.; Pak, K.; Chavez, E.; Ryan, A. F. *Neuroscience* **2010**, *166*, 1185.
- (42) Izumikawa, M.; Minoda, R.; Kawamoto, K.; Abrashkin, K. A.; Swiderski, D. L.; Dolan, D. F.; Brough, D. E.; Raphael, Y. *Nat. Med.* **2005**, *11*, 271.
- (43) Thompson, D. B.; Cronican, J. J.; Liu, D. R. In *Methods in Enzymology*; Wittrup, K. D., Gregory, L. V., Eds.; Academic Press: Waltham, MA, 2012; Vol. 503, p 293.
- (44) Simons, S. S.; Pons, M.; Johnson, D. F. *J. Org. Chem.* **1980**, *45*, 3084.
- (45) Dunkerton, L. V.; Markland, F. S.; Li, M. P. *Steroids* **1982**, *39*, 1.
- (46) Kwon, Y. U.; Kodadek, T. *J. Am. Chem. Soc.* **2007**, *129*, 1508.
- (47) Sage, C.; Huang, M.; Karimi, K.; Gutierrez, G.; Vollrath, M. A.; Zhang, D.-S.; García-Añoveros, J.; Hinds, P. W.; Corwin, J. T.; Corey, D. P.; Chen, Z.-Y. *Science* **2005**, *307*, 1114.